Regional Strain Variations in the Human Patellar Tendon

STEPHEN J. PEARSON[1], TIM RITCHINGS[2], and AZLAN S.A. MOHAMED[2]

[1]Centre for Health, Sport and Rehabilitation Sciences Research, University of Salford, Greater Manchester, UNITED KINGDOM; and [2]Control & Systems Engineering Research Centre, University of Salford, Greater Manchester, UNITED KINGDOM

ABSTRACT

PEARSON, S. J., T. RITCHINGS, and A. S. MOHAMED. Regional Strain Variations in the Human Patellar Tendon. *Med. Sci. Sports Exerc.*, Vol. 46, No. 7, pp. 1343–1351, 2014. **Purpose**: Characteristics of localized tendon strain *in vivo* are largely unknown. The present study examines local tendon strain between the deep, middle, and surface structures at the proximal and distal aspects of the patellar tendon during ramped isometric contractions. **Methods**: Male subjects (age 28.0 ± 6.3 yr) were examined for patellar tendon excursion (anterior, midsection, and posterior) during ramped isometric voluntary contractions using real-time B-mode ultrasonography and dynamometry. Regional tendon excursion measurements were compared using an automated pixel tracking method. Strain was determined from the tendon delta length normalized to initial/resting segment length. **Results**: Strain increased from 10% to 100% of force for all regions. Significantly greater mean strain was seen for the anterior proximal region compared to the posterior and mid layer of the tendon (7.5% ± 1.1% vs 3.7% ± 0.5% vs 5.5% ± 1.0%; $P < 0.05$). Similarly, the distal posterior region showed greater mean strain compared to the mid and anterior regions (7.9% ± 0.6% vs 5.0% ± 0.6% vs 5.4% ± 0.6%; $P < 0.05$). Relative changes in strain differences from 50% to 100% of force for the proximal region were greatest for the anterior to midline regions (4.6% ± 0.6% and 5.6% ± 0.6%, respectively) and those for the distal region were also greatest for the anterior to midline regions (4.4% ± 0.2% and 5.3% ± 0.2%, respectively). The largest mean strain for the proximal region was at the anterior layer (7.5% ± 1.1%) and that for the distal tendon region was at the posterior layer (7.9% ± 0.9%). **Conclusions**: This study shows significant regional differences in strain during ramped isometric contractions for the patellar tendon. Lower proximal strains in the posterior tendon compared to the anterior region may be associated with the suggestion of "stress shielding" as an etiological factor in insertional tendinopathy. **Key Words:** *IN VIVO*, TENDON, REGIONAL STRUCTURAL PROPERTIES, ULTRASOUND

The tendon is described as a viscoelastic structure and has been shown to have characteristic strain approximating linearity over a range of physiological loading (28). With increased strain, there is a risk of damage to the tendon structure, leading to tears and ultimately rupture. Previous *in vivo* work using noninvasive ultrasound imaging has described the patellar tendon properties in terms of its stiffness (extension per unit load) and associated strain values during voluntary contractions (5,10,27). However, previous works have limitations in that the methods used to determine the values shown are in relation to the whole tendon and, as such, do not represent the mechanical properties of discrete portions of the tendon. Indeed, previous studies have highlighted the nonuniform nature of the human tendon with respect to the cross-sectional area (11,12,15,24). Assuming similar forces in the tendon, this would indicate that the stress (force per unit area) is different along the tendon structure. If the tissue is homogenous then the strain may well be region specific. However, it may be that the loading is not homogenous along the tissue and that the strain may indeed be equivalent in line with the differences in the cross-sectional area. In any case, if the strain is not uniform, it may indicate shear loading that could lead to excessive microtrauma or tears and cumulative damage of the tendon structure.

Tendon-like muscle is able to alter its mechanical properties in response to loading. It comprises mainly of collagen fibrils and of which the predominant form is Type I. These collagen fibrils play a major role in the characteristic mechanical properties of the tendon. It is known that collagen turnover is responsive to loading and will increase or decrease its turnover rates accordingly. The effect of increased loading and concomitant increased tendon collagen has been shown previously in animals (17) and also in humans in response to acute (25) and chronic exercise (19,32).

Recently, Hansen et al. (11) showed that tendon fascicles from the anterior tendon were in fact stiffer and stronger with less mature pyridinium-type cross-links relative to fascicles from the posterior tendon region. These data, however, were

Address for correspondence: Stephen J. Pearson, Ph.D., Sport, Exercise & Physiotherapy, University of Salford, Manchester M66PU, United Kingdom; E-mail: s.pearson@salford.ac.uk.
Submitted for publication April 2013.
Accepted for publication December 2013.

0195-9131/14/4607-1343/0
MEDICINE & SCIENCE IN SPORTS & EXERCISE®

DOI: 10.1249/MSS.0000000000000247

from anterior cruciate ligament surgery patients, and it is not known to what degree these would be representative of the "normal" population. Despite this suggested greater resistance to strain of the anterior tendon, because of the lever arm arrangements of the patellar relative to the tendon, it may well be that forces are greatest at the anterior region because of the lever arm advantage at the patellar surface in comparison to the deep layers leading to increased strain for a given external force. It is not unreasonable to assume that the tissue that is metabolically active could be nonhomogenous in terms of the collagen turnover rates, leading to potential regional differences in mechanical properties. For example, recently, Couppé et al. (9) reported differential hypertrophy of the patellar tendon along its length in comparison to the contralateral (i.e., nondominant) tendon in athletes who had a tendency to display a dominant limb. Similarly, in human subjects, Carroll et al. (7) reported regional differences in tendon cross-sectional area (CSA) with the proximal patellar tendon showing greater CSA compared to the mid and distal regions.

It has previously been suggested that the patellar tendon is "differentially" stimulated during loading, leading to "overuse" type problems as in tendinopathy (23). This pattern is seen often at the proximal posterior portion of the patellar tendon. Of the few studies carried out examining regional patellar strain in cadaveric knee flexion models, one reported greater anterior strain; in contrast, the other stated the posterior portion experienced greater strain (1,3).

Tendinopathies have been described as being associated with overuse, where continued excessive loading leads to eventual tendon degradation via accumulated microdamage (20). However, "stress shielding" has been suggested as an alternative explanation for the development of tendinopathy (23). Where insertional tendinopathies are seen, there is a tendency for the pathology to occur at the posterior or joint side of the tendon. Here cartilaginous metaplasia can be seen to occur (34), typical with compressive loading, suggestive of nonuniform strain or loading across the tendon. These tendon-related anomalies are seen to be implicated in an increasing number of tendon-related functional disabilities in both the sporting and nonathletic populations and which have a tendency to become chronic and degenerative. Understanding of the etiology of tendinopathies is poor, and as such, treatment and rehabilitation modalities are not well defined.

The method described here allows for the quantification of the mechanical properties of the tendon at discrete regions of interest within the intact tendon structure. Thus, it may allow for the sensitive identification of patterns of strain and associated changes within the tendon before injury, during rehabilitation or with disease, which cannot be identified using the method outlined in previous work. Detailed characterization of the tendon may allow for further insight into the etiology of tendon injury, repair, and response to various training interventions.

Because of the previous observations and suggestions of differential loading of tendon structures, we hypothesize that, under ramped maximal isometric loads, the patellar tendon will show regional differences in strain between the deep and superficial layers and that the proximal and distal tendon will exhibit characteristic differences in strain patterns.

Therefore, the purpose of this present study was to examine proximal and distal localized strain across the anterior, mid, and posterior aspects of the patellar tendon using automated speckle tracking of dynamic ultrasound images of *in vivo* human patellar tendon tissue during ramped isometric loading.

By describing the regional tendon mechanical properties, the ultimate objective of this work was to initiate a much more detailed understanding of the tendon in injury, in repair, and also in response to various training interventions. This detailed understanding will allow for more effective screening, rehabilitation, and injury prevention strategies to be put in place.

METHODS

Subjects and experimental design. Sixteen healthy limbs were used for data collection in this study from healthy male subjects (age 28.0 ± 6.3 yr, height 1.7 ± 0.04 m, and body mass 79 ± 5.4 kg). The local ethics committee approved the investigation, and all participants gave written informed consent to participate. The study conformed to the principles of the World Medical Association's Declaration of Helsinki.

A 7.5-MHz 100-mm linear array, B-mode ultrasound probe (Mylab 70; Esaote Biomedica, Italy) with a depth resolution of 67 mm was used to image the patellar tendon in the sagittal plane, and the knee was fixed at 90° flexion. Ultrasound images were then taken in DV output and captured at 25 frames per second. Scaling in pixels per millimeter was determined from ImageJ software by using the known depth of field in the ultrasound images (1 mm = 11 pixels in the x and y directions) and used as a calibration factor in the automated tracking program to ensure equivalent pixel-to-millimeter ratios.

The tendon was imaged during ramped voluntary contractions where the transducer probe was fixed statically at the skin surface. Torque output during isometric quadriceps contraction was determined using a dynamometer (Type 125 AP; Kin Com, Chattanooga, TN), with the participant in a seated position. The knee was fixed at 90° flexion (full extension = 0°) and hip at 85° (supine = 0°), and a lever attachment cuff was placed on the lower leg at ~3 cm above the medial malleolus. Three maximal isometric quadriceps contraction efforts were carried out to ensure tendon preconditioning before the test. Participants were instructed to perform ramped isometric contractions from rest to maximum over a 3- to 4-s period. Three trials of the knee extension test were performed with 180 s of rest between contractions. Mean values of strain for the three contractions for each individual were used for subsequent analysis. The

ultrasound output was synchronized (using an electronic square wave signal generator) with the torque records to allow temporal alignment. EMG determined any cocontraction that was added to the net knee extension torque to give total torque. The EMG of the long head of the biceps femoris muscle (BF) was measured to ascertain the level of antagonistic muscle cocontraction during the isometric knee extension (29). Assumptions were that BF is representative of its constituent muscle group (4) and that the BF EMG relationship with knee flexor torque is linear (21). Briefly, a series of three maximal isometric knee flexion contractions were carried out to obtain the EMG at maximal flexion torque. The root mean square EMG activity corresponding to the peak torque period was analyzed over 50-ms epochs and was averaged for a 1-s period during the plateau of peak torque. This has previously been suggested to be acceptable in terms of signal-to-noise ratio (13). The EMG activity of the BF during knee extension was divided by the maximal flexor EMG, and the maximal flexor torque was then multiplied by this value to determine cocontraction torque.

The patellar tendon force was then determined by dividing the total torque by the patellar lever arm, determined from the literature (18,33). Captured grayscale ultrasound images gave regional attributes (dimensions, position coordinates, and grayscale pixel values). In the compared frame, the coordinates of the region of interest (ROI) were offset along the horizontal and vertical image planes and were shifted by a pixel at a time.

Tracking algorithm. To date, there are limited numbers of validated techniques to measure discrete tissue movement *in vivo* without the use of identifiable landmarks (9). Block matching techniques to measure tissue movement have been used previously (8,22,26). Dilley et al. (10) have also shown that an optical flow technique can be used to study tissue displacement. However, optical flow performs better with smaller frame-to-frame displacements compared to speckle tracking. The design of tracking algorithms requires the capability of the algorithm to handle both small and large frame-to-frame displacements to maintain accuracy. Where monitoring of tendon displacement during voluntary contractions is required, there are a number of ways to reduce frame-to-frame displacement; either ensure the ramped contraction is slow enough to reduce frame-to-frame displacement for a given frame rate or increase the frame acquisition rate to give a smaller frame-to-frame displacement (30). The regional block is needed to capture a unique speckle pattern; this is important because tendons have a typical striated speckle pattern when compared to other tissue areas. The size of the ROI block has to be optimal: a relatively smaller block is less susceptible to deformation

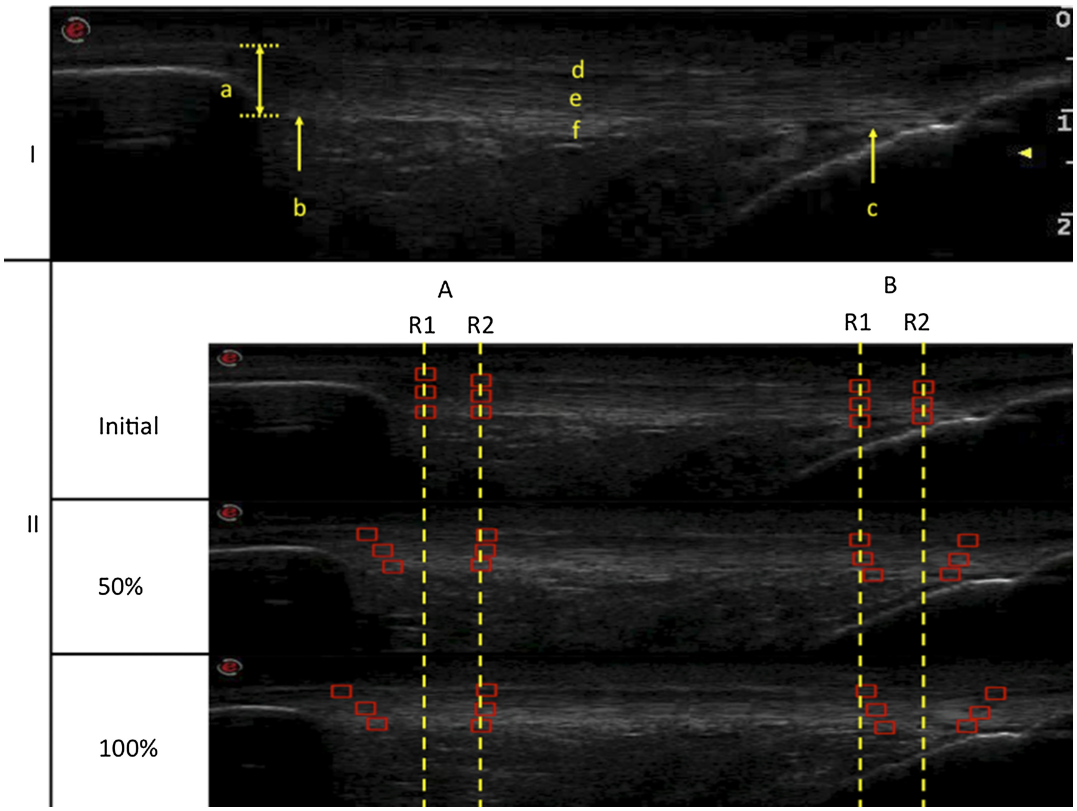

FIGURE 1—(I) Example ultrasound image illustrating the tendon area investigated. The thickness of the tendon is on average of 8–9 mm (a). The tendon regions investigated are proximal (b) and distal (c) ends. The regional layers for each tendon end are divided into boundaries of anterior (d), mid (e), and posterior (f). The bone structures are clearly seen at both end, and the thin layer at the top of the image is the skin layer (i). (II) Regional tracking of ROIs where R_1 and R_2 are the arbitrary pixel regions in the tendon arranged into layers on a typical tendon excursion on both proximal (A) and distal (B) ends showing shift in the ROIs from the resting tendon at 50% and 100% force. The *dotted lines* show the initial positions of the ROIs.

but local artifacts with an ambiguous pattern may be seen, whereas larger blocks may contain a less ambiguous and unique pattern, but during rapid motion, the pattern in the block may deform more, leading to a lower correlation (30). The previous work by Pearson et al. (33) validates the methods used here to follow discrete regions of the tendon during maximal isometric contractions.

A block matching algorithm using normalized cross-correlation (NCC) (Eq. [1]) was used as the search schema to determine the similarity between subsequent frames. The tendon was arranged into three layers at the proximal and distal ends (Fig. 1). Multiple search blocks (ROIs) were placed manually on the regional layers of the tendon at both ends (Fig. 1). These were then used to determine the relative excursion from the initial start point and also to calculate the strain at the specific force levels. An optimal ROI size was used (15 × 15 pixel based on previous work [30]) to track multiple layers of the tendon with the search window for each ROI fixed at 2 × ROI size for the width and at 1 × ROI size for the height. Multiple ROIs of the same size as the initial ROIs are distributed along the selected ROI layers to calculate the average displacements to help improve the accuracy during frame-to-frame tracking. For frame-to-frame movements of the ROI, within each search window, the ROIs were displaced by 1 pixel at a time compared with the original ROI in the previous frame and were evaluated using NCC, the results of which are stored in a matrix and best matches based on peak detection (i.e., the highest correlation value). To reduce the chances of decorrelation, the correlation threshold value was set to ≥0.9. If the threshold value was not reached or exceeded then the ROI was not moved in the subsequent frame. Otherwise, the tracking would start with the new, updated position of the template ROI blocks in the next frame.

$$\rho_{\mathrm{nm(k,l)}} = \frac{\sum_{i=-K}^{K}\sum_{j=-L}^{L}[F_1(n+i,m+j)F_2(n+k+i,m+l+j)]}{\left[\sum_{i=-K}^{K}\sum_{j=-L}^{L}[F_1(n+i,m+j)]^2\right]^{1/2}\left[\sum_{i=-K}^{K}\sum_{j=-L}^{L}[F_2(n+k+i,m+l+j)]^2\right]^{1/2}} \quad [1]$$

where F_1 refers to the image block of the initial frame and F_2 is the image block of the subsequent frame. Coordinate (n,m) is the center of the image block and the sum is over (i,j), whereas (k,l) refer to the displacements in the lateral and axial directions. $\rho_{nm(k,l)}$ represents the normalized correlation ranging from −1 to 1 and 1 being the closest match.

The test is composed of two regions of interests (2-ROI) R_1 and R_2 (Fig. 1) tracked from the initial frame to the last frame. The determined measurement of the displacement is the difference of the distance of two nodes at 10% intervals of force up to 100% MVC. For all repeat trials (three), the initial positions of the ROIs were the exact same reference points in the frame.

The measurements taken for the tests are classified into six parts: proximal anterior tendon excursion (PS), proximal midline tendon excursion (PM), proximal posterior tendon excursion (PP), also distal anterior tendon excursion (DS), distal midline tendon excursion (DM), and distal posterior tendon excursion (DP). The movement in each layer for each frame is determined by measuring the distance of x and y for both R_1 and R_2 regions from the initial frame (f_1) to frame (f_n). The resulting displacement for each layer is measured by subtracting the initial frame (f_1) distance from the frame (f_n) as formulated in Arndt et al. (2). Strain measurement is thus the displacement (defined in Eq. [2]) divided by the initial distance between R_1 and R_2. All initial proximal and distal regions were aligned vertically to enable quantification of any differences in regional strain within a localized site of the tendon.

$$\mathrm{Disp} = \left(\sqrt{(x_{R2}-x_{R1})^2+(y_{R2}-y_{R1})^2}\right)_{fn} - \left(\sqrt{(x_{R2}-x_{R1})^2+(y_{R2}-y_{R1})^2}\right)_{f1} \quad [2]$$

Statistics. Intraclass correlation coefficients (ICCs) were determined to examine the reliability/robustness of the measures by carrying out repeated tracking on the full data set at each 10% increment of force. Between-region comparisons (all regions being independent) for all strain (dependant variable) measures (at given levels of force at 10% increments) were carried out using two-way ANOVA and Bonferroni *post hoc* pairwise tests. The α level was set to $P = 0.05$. All data are presented as mean ± SEM. Sample size was determined using G power (3.09, Franz, Faul, Universitat, Keil, Germany). For a power $(1 - \beta)$ of 0.95 and a moderate effect size of 0.2, a sample size of 15 was calculated.

RESULTS

Reliability. Repeat tests of the measures for tendon excursion at all layers and forces gave an ICC of 0.9. Percentage cocontraction was determined at MVC using EMG to examine the possibility of cross-talk from the quadriceps muscle. A mean ± SEM value of 6.9% ± 0.5% was seen indicating low cocontraction at maximal levels of agonist activity.

Proximal tendon strain. All layers showed increased strain across the force levels from 10% to 100% ($P < 0.01$) (Fig. 2). Levels of absolute force and the interindividual variability at each percentage of force level can be seen in Table 1A. The analysis also revealed an interaction of force by layer. Subsequent one-way ANOVA showed no significant difference ($P > 0.05$) at force levels of 50%–60% and 90%–100% for the anterior layer and no significant difference ($P > 0.05$) at force levels of 40%–60% for the mid layer. The posterior layer showed no significant difference ($P > 0.05$) at force levels of 30%–60% and 70%–100%.

Distal tendon strain. Similar to the proximal strain, it can be seen in Figure 3 that all distal layers showed increased strain across the force levels from 10% to 100%. Analysis revealed a significant increase in strain with force ($P < 0.01$); the mean strain values for the posterior layer were seen to be greater than those for both anterior ($P = 0.01$) and midline regions ($P < 0.01$) (7.9% ± 0.6% vs 5.4% ± 0.6%

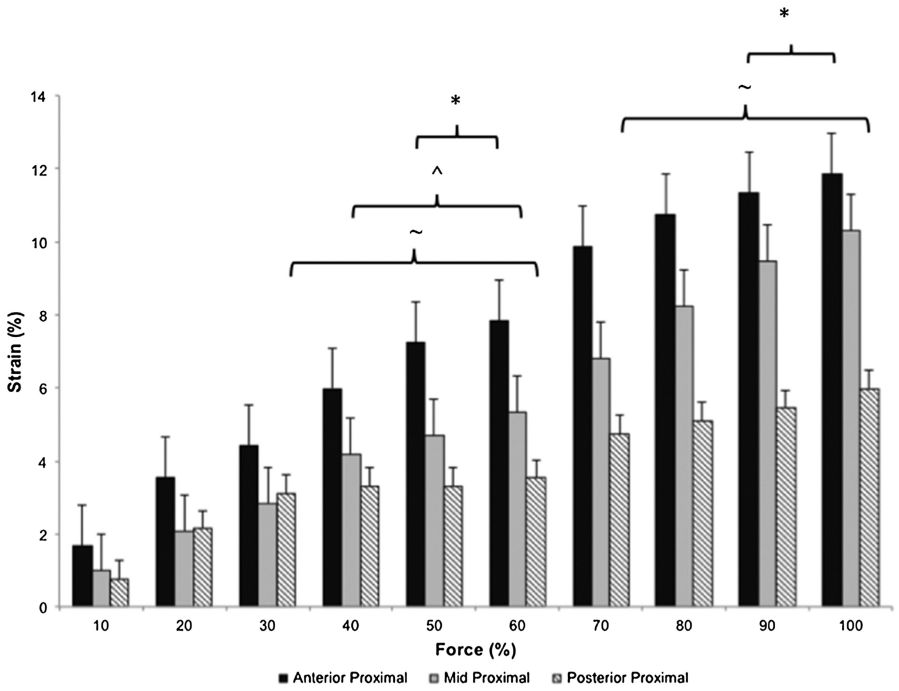

FIGURE 2—Strain values for all measured proximal regions (mean ± SEM) at 10%–100% MVC. *Mean strain of the anterior layer shows no significant differences ($P > 0.05$) at the force levels. ~Mean midline shows no significant differences ($P > 0.05$) at force levels. ^Mean posterior layer shows no significant differences ($P > 0.05$) at force levels.

and 5.0% ± 0.6%, respectively). No interaction between layer and force was shown.

Figure 4 illustrates instantaneous regional strain values at 50% and 100% of force. Total mean strain (all regions) was greater at 100% compare to that at 50% strain (9.8% ± 0.8% vs 5.3% ± 0.7%; Table 1B). No interaction was seen between force level and region ($P > 0.05$). Pooled values (50% and 100%) indicated that strains at the proximal anterior and distal posterior regions were greater than those at all other regions ($P < 0.05$). Strain at the proximal midline region was also significantly different from that at the proximal posterior region (Table 1B).

Proximal anterior and distal posterior regions were seen to have significantly greater mean strain than all other regions (7.5% ± 1.1% and 7.9% ± 0.9%, respectively, $P < 0.05$). Also, the distal anterior region showed greater mean strain in

TABLE 1. Absolute forces (mean ± SD) at each percentage of maximum (A) and instantaneous strain values at 50% and 100% with its relative difference and corresponding pooled mean values for each layer at both proximal and distal regions of the patellar tendon.

(A)

	Tendon Force (N)		
MVC (%)	**Min**	**Max**	**Mean**
10	1053	1225	1034 ± 16
20	1851	2315	1918 ± 22
30	2958	2944	3290 ± 124
40	4166	3909	3761 ± 47
50	5011	4850	4654 ± 63
60	6143	6002	5560 ± 71
70	7560	6711	6491 ± 85
80	8221	7565	7437 ± 91
90	9443	8800	8344 ± 104
100	10177	9725	9185 ± 117

(B)

	Strain						
	Proximal			Distal			
Force (%)	**Anterior**	**Midline**	**Posterior**	**Anterior**	**Midline**	**Posterior**	**Total Mean Strain**
50	7.2 ± 0.5	4.7 ± 0.9	3.3 ± 0.6	4.6 ± 0.7	4.3 ± 0.7	7.8 ± 0.9	5.3 ± 0.7
100	11.9 ± 0.6	10.3 ± 0.7	6.0 ± 0.9	9.0 ± 0.9	9.6 ± 0.8	12.0 ± 0.7	9.8 ± 0.8
Difference	4.7 ± 0.1	5.6 ± 0.2	2.7 ± 0.3	4.4 ± 0.2	5.3 ± 0.1	4.2 ± 0.2	
Pooled mean value	9.6 ± 0.6	7.5 ± 0.8	4.7 ± 0.8	6.8 ± 0.8	7.0 ± 0.8	9.9 ± 0.8	

For part A, ranges of force observed at each percentage level are also presented.
For part B, total mean strain represents the average strain over all regions at both 50% and 100% force. These differences in strain between 50% and 100% could indicate shear between the tendon boundary layers.

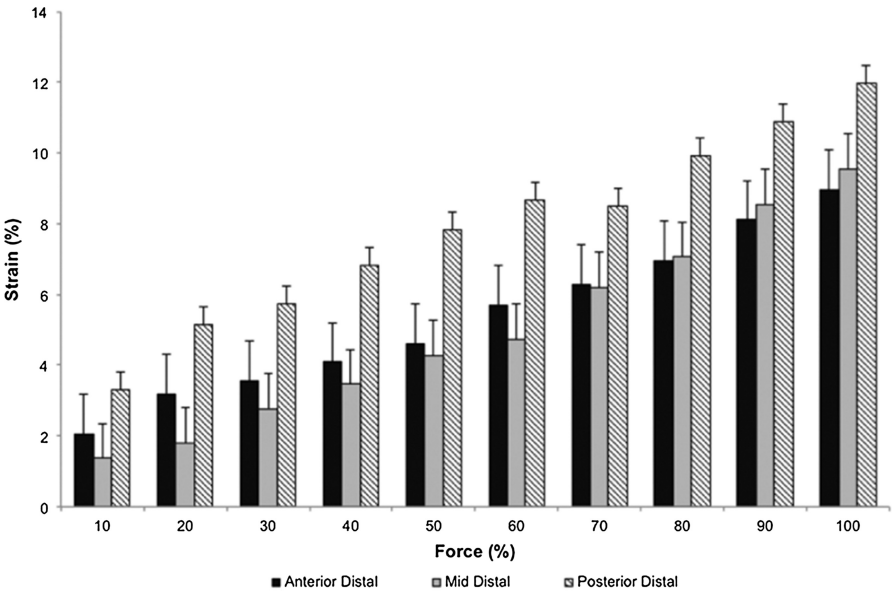

FIGURE 3—Distal mean strain significantly increased with force level ($P < 0.01$). Mean anterior strain was greater than posterior strain ($P = 0.01$). Mean midline strain was also greater than the mean posterior strain ($P < 0.01$).

comparison to the proximal posterior region (5.5% ± 1.0% vs 3.7% ± 0.5%, respectively, $P = 0.02$; Fig. 5).

DISCUSSION

The current study aimed to examine and compare localized proximal strain at both the anterior and posterior regions of the patellar tendon. The findings show that, in the patellar tendon of a group of healthy young subjects, the greatest mean strains during isometric ramped contractions were seen in the anterior layer at the proximal end (7.5%) and in the posterior layer at the distal end (7.9%; Fig. 5). Of particular interest was the finding that for the proximal and distal regions of the tendon, there were significant differences between the layers of the tendon examined.

Previous studies have validated the use of localized tracking of the tendon using block matching techniques similar to that used here (14,16,31). Korstanje et al. (16) reported relatively small errors of up to 1.6% when attempting to track an *in vivo* structure. Here we also show very good repeatability of tracking data, indicating very good agreement with other reports of measurement. A recent study (9) reported that the speckle tracking method was able to estimate frame-to-frame displacements using 2-ROI end

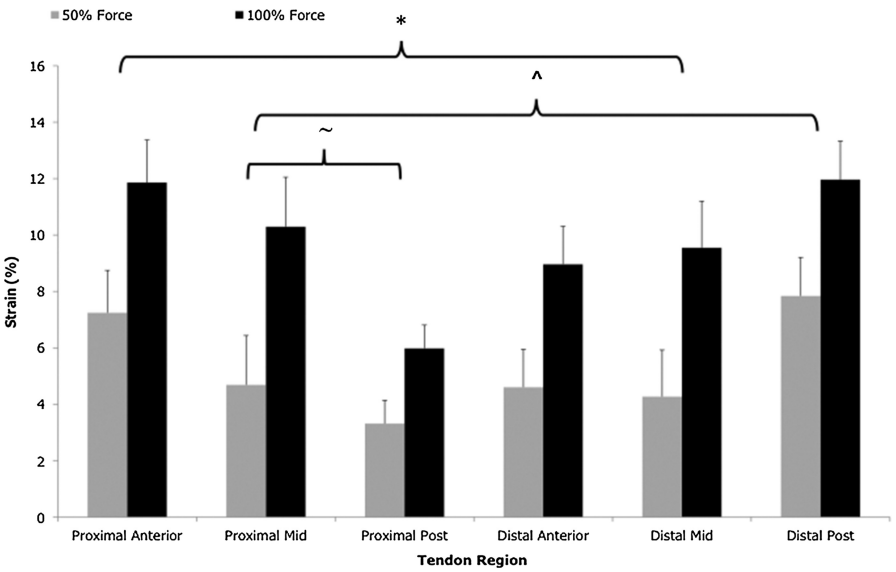

FIGURE 4—Instantaneous strain values for all layers at both proximal and distal regions of the patellar tendon at 50% and 100% force. *Pooled mean strain of the proximal anterior region was significantly different from regions other than the distal posterior region (*$P < 0.05$). ^Pooled mean strain of the distal posterior region was significantly different from regions other than the proximal anterior region ($P < 0.05$). ~Pooled mean strain of the proximal posterior region was significantly different from the distal anterior region ($P = 0.06$).

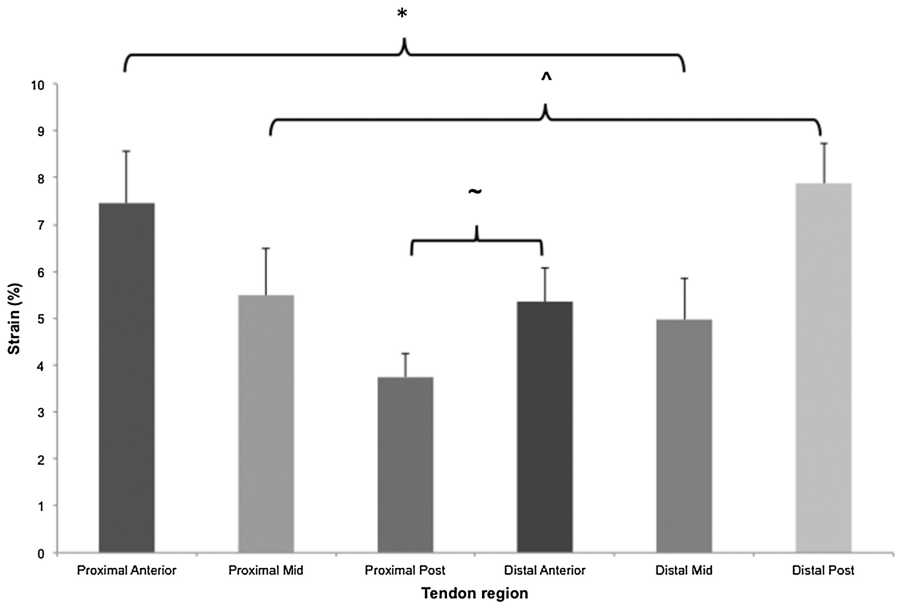

FIGURE 5—Mean strain (10%–100%) for all layers at both proximal and distal regions of the patellar tendon. *Mean strain at the proximal anterior region was significantly different from regions other than the distal posterior region ($P < 0.05$). ^Mean strain at the distal posterior region is significantly different from regions other than the proximal anterior region ($P < 0.01$). ~Mean strain at the proximal posterior region was significantly different from the distal anterior region ($P = 0.02$).

points by tracking the movement of the tendon during twitch contractions. However, because the tracking was carried out during twitch contractions by electrically stimulating the muscle, the forces in the tendon were only moderate (up to 50% of maximum), which is a major difference to the approach here where high forces were elicited (see Table 1 for levels of absolute forces), and thus larger tendon deformations would be expected, making tracking more difficult. In addition, a previous work has indicated that contraction time can affect the amount of excursion seen in the tendon (28); this can be explained as caused by the viscoelastic nature of the tendon. It could then be speculated that the composition of the tendon at different regions may be proportionally different in terms of the viscous and elastic components, which would affect the time course of extension under load to different degrees.

The determined mean strains reported here at MVC (~7.5%–7.9%) for the tendon were within the range of those reported for this structure in young males (5,10,27), with these previous references showing a range of 6%–10.6%. The anterior and posterior regional strains have been previously reported in cadaveric specimens (3); here, strain values at a load of 1 kN were 1.7% and 3.2% for the anterior and posterior regions, respectively. In the present study, we report strain values of 7.5% and 3.7% for the proximal anterior and posterior tendon regions, whereas distal anterior and posterior regions show 5.4% and 7.9% tendon strain, respectively (Fig. 5), which are considerably larger than those reported by Basso et al. This may in part reflect differences in the level of load and the application of load and also that the strain was determined in the proximal and distal sections of the tendon compared to the mid third used by Basso et al. It may be that the tendon is not homogenous throughout its length and could be structurally different in terms of the collagen content, collagen type, and extracellular matrix density. In addition to this, the samples used by Basso et al. were from cadavers and these may not have accurately reflected the values for "live" tissues as measured here.

Others have also indicated that regional layer differences exist in strain within a tendon. A study using speckle tracking to estimate *in vivo* tendon strain, examining layer differences in strain of the supraspinatus tendon during isometric and isotonic efforts, reported that the superficial layer of the tendon showed greater strain relative to the deep layers (14). Also during passive plantar dorsi flexion of the ankle, it was seen that the Achilles tendon showed greater relative displacement of the deep portion of the tendon in comparison to the superficial and mid portions (2).

Indeed, Almekinders et al. (1) showed larger forces/strains present in cadaveric patellar specimens on the anterior portion of the proximal tendon. In intact human muscle/tendon systems, however, there is the complex interplay of agonist–antagonist interaction and differences in the mechanical tissue properties to that of cadaveric specimens. Any differences in the applied force, if it is habitual, should lead to adaptation of the structures under normal circumstances.

In relation to the distal tendon, it has been observed previously (unpublished observations by authors) that the tibial insertion end rotates inward (posterior) in the sagittal plane when forces are generated in the protocol as used here. Thus, this "twisting" of the bone attachment could partly cause the differential strain as seen here, both between the proximal and distal ends and the layers of the distal end. These different patterns of strain between the tendon layers at the sites measured could indicate shear of the tendon structure. For

example, we clearly show greater strain in the anterior region for the proximal tendon and in the posterior region for the distal tendon. In addition, the relative strain change (within layers) with increased loading (from 50% to 100%; Fig. 4) force again indicated the probability of shear between the tendon layers, as each region strain is different at given force levels, thus causing differential longitudinal movement between layers (shear force). In time, this relative difference in strain at different levels of force may in fact be a factor in the development of cumulative tendon injury. In addition, all the above reported measures of *in vivo* tendon properties have been carried out at a knee angle of 90°; it would be interesting to determine local tissue strains at a number of different knee angles to identify whether the ratios of local strains are similar to that at 90°. This would present a useful insight into perhaps a more functional interpretation of the localized strains as reported here. Bojsen-Moller et al. (5) showed that, during plantarflexion with the knee either straight or bent to 90°, there was differential strain in the aponeuroses of the gastrocnemius and soleus, thus indicating a potential for "shear" between these structures, with a functional change in segment angle. Others have also observed differential forces across the tendon structure during loading. Arndt et al. (3) reported different loading on either side of the Achilles tendon dependent on which muscles of the lower limb were activated. On the other hand, Lersch et al. (23) reported in cadaveric specimens that Achilles tendon strain differentials of up to 15% were observed by changes in the calcaneous position. However, here we would also draw attention to the understanding that statistical significance alone does not constitute "clinical" or physiological significance, and future studies will have to elucidate this further.

Tendinopathies have been reported to alter the mechanical properties of the tendon. Child et al. (8) reported an increased compliance of the Achilles tendon aponeurosis in a group of runners with midportion tendinopathy. If changes such as this are seen with specific degenerative states or diseases, it can be seen that a sensitive marker for changes in localized tendon strain may be very useful as a predictor of disease/degeneration progression. Indeed, with further testing, patterns of "change," or indicators of "risk," may be developed to help early intervention or rehabilitation of damaged tendon.

CONCLUSIONS

The method used here has the potential to improve clinical knowledge relating to the tendon's mechanical properties. It is clear that the strain throughout the tendon structure is not equal for a given external force, lending itself to tissue shear and hence to potential increased injury risk in specific areas of the tendon. Future studies using this methodology will include testing of other tendon landmarks to determine and describe discrete tendon mechanical properties and to examine various changes in regional tendon stiffness and strain in relation to sex, age, and specific disease states (i.e., tendinopathies, diabetes). It is for future studies to determine how and why these differences in strain may affect the etiology of the disease and to determine the effects of training rehabilitation. These studies will give further insight into the etiology of tendon injury, repair, response to various training interventions, and the time course of tissue adaptation with disease.

The authors thank all study participants without whom none of this work would have been possible.

No funding was received for any part of this work.

The authors are not professionally and/or financially affiliated to any institution that may be perceived as causing a bias in the presentation of their results. Results of the present study do not constitute endorsement by the American College of Sports Medicine.

REFERENCES

1. Almekinders LC, Vellema JH, Weinhold PS. Strain patterns in the patellar tendon and the implications for patellar tendinopathy. *Knee Surg Sports Traumatol Arthrosc*. 2002;10(1):2–5.
2. Arndt A, Bengtsson AS, Peolsson M, Thorstensson A, Movin T. Non-uniform displacement within the Achilles tendon during passive ankle joint motion. *Knee Surg Sports Traumatol Arthrosc*. 2011:1868–74.
3. Arndt A, Bruggemann GP, Koebke J, Segesser B. Asymmetrical loading of the human triceps surae: I. Mediolateral force differences in the Achilles tendon. *Foot Ankle Int*. 1999;20:444–9.
4. Basso O, Amis AA, Race A, Johnson DP. Patellar tendon fiber strains: their differential responses to quadriceps tension. *Clin Orthop Relat Res*. 2002;(400):246–53.
5. Bojsen-Moller J, Hansen P, Aagaard P, Svantsson U, Kjaer M, Magnusson P. Differential displacement of the human soleus and medial gastrocnemius aponeuroses during isometric plantar flexion contractions *in vivo*. *J. Appl Physiol*. 2004;97:1908–14.
6. Carolan B, Cafarelli E. Adaptations in coactivation after isometric resistance training. *J Appl Physiol*. 1992;73(3):911–7.
7. Carroll CC, Dickinson JM, Haus JM, et al. Influence of aging on the *in vivo* properties of human patellar tendon. *J Appl Physiol*. 2008;105(6):1907–15.
8. Child S, Bryant AL, Clark RA, Crossley KM. Mechanical properties of the Achilles tendon aponeurosis are altered in athletes with Achilles tendinopathy. *Am J Sports Med*. 2010;38(9):1885–93.
9. Couppé C, Kongsgaard M, Aagaard P, et al. Habitual loading results in tendon hypertrophy and increased stiffness of the human patellar tendon. *J Appl Physiol*. 2008;105(3):805–10.
10. Dilley A, Greening J, Lynn B, Leary R, Morris V. The use of cross-correlation analysis between high-frequency ultrasound images to measure longitudinal median nerve movement. *Ultrasound Med Biol*. 2001;27(9):1211–8.
11. Farron J, Varghese T, Thelen DG. Measurement of tendon strain during muscle twitch contractions using ultrasound elastography. *IEEE Trans Ultrason Ferroelectr Freq Control*. 2009;56(1):27–35.
12. Hansen P, Bojsen-Moller J, Aagaard P, Kjaer M, Magnusson SP. Mechanical properties of the human patellar tendon, *in vivo*. *Clin Biomech (Bristol, Avon)*. 2006;21(1):54–8.
13. Hansen P, Haraldsson BT, Aagaard P, et al. Lower strength of the human posterior patellar tendon seems unrelated to mature collagen cross-linking and fibril morphology. *J Appl Physiol*. 2010;108(1):47–52.

14. Haraldsson BT, Aagaard P, Krogsgaard M, Alkjaer T, Kjaer M, Magnusson SP. Region-specific mechanical properties of the human patella tendon. *J Appl Physiol*. 2005;98(3):1006–12.
15. Hermens HJ, Fredriks B, Disselhorst-Klug C, Rau G. Development of recommendations for SEMG sensors and sensor placement procedures. *J Electromyogr Kinesiol*. 2000;10(5):361–74.
16. Kim YS, Kim JM, Bigliani LU, Kim HJ, Jung HW. *In vivo* strain analysis of the intact supraspinatus tendon by ultrasound speckles tracking imaging. *J Orthop Res*. 2011;29(12):1931–7.
17. Kongsgaard M, Reitelseder S, Pedersen TG, et al. Region specific patellar tendon hypertrophy in humans following resistance training. *Acta Physiol (Oxf)*. 2007;191(2):111–21.
18. Korstanje JW, Selles RW, Stam HJ, Hovius SE, Bosch JG. Development and validation of ultrasound speckle tracking to quantify tendon displacement. *J Biomech*. 2010;43(7):1373–9.
19. Kovanen V, Suominen H. Age and training-related changes in the collagen metabolism of rat skeletal muscle. *Eur J Appl Physiol Occup Physiol*. 1989;58(7):765–71.
20. Krevolin JL, Pandy MG, Pearce JC. Moment arm of the patellar tendon in the human knee. *J Biomech*. 2004;37(5):785–8.
21. Kubo K, Ikebukuro T, Maki A, Yata H, Tsunoda N. Time course of changes in the human Achilles tendon properties and metabolism during training and detraining *in vivo*. *Eur J Appl Physiol*. 2012;112(7):2679–91.
22. Leadbetter WB. Cell–matrix response in tendon injury. *Clin Sports Med*. 1992;11(3):533–78.
23. Lersch C, Grötsch A, Segesser B, Koebke J, Brüggemann GP, Potthast W. Influence of calcaneus angle and muscle forces on strain distribution in the human Achilles tendon. *Clin Biomech (Bristol, Avon)*.2012;27(9):955–61.
24. Lippold OC. The relationship between integrated action potentials in a human muscle and its isometric tension. *J Physiol*. 1952; 177:492–9.
25. Loram ID, Maganaris CN, Lakie M. Use of ultrasound to make noninvasive *in vivo* measurement of continuous changes in human muscle contractile length. *J Appl Physiol*. 2006;100(4): 1311–23.
26. Maganaris CN, Narici MV, Almekinders LC, Maffulli N. Biomechanics and pathophysiology of overuse tendon injuries: ideas on insertional tendinopathy. *Sports Med*. 2004;34(14):1005–17.
27. Magnusson SP, Kjaer M. Region-specific differences in Achilles tendon cross-sectional area in runners and non-runners. *Eur J Appl Physiol*. 2003;90:549–53.
28. Miller BF, Olesen JL, Hansen M, Døssing S, Crameri RM, Welling RJ. Coordinated collagen and muscle protein synthesis in human patella tendon and quadriceps muscle after exercise. *J Physiol*. 2005;15(567):1021–33.
29. Ofer N, Akselrod S, Nyska M, Werner M, Glaser E, Shabat S. Motion-based tendon diagnosis using sequence processing of ultrasound images. *J Orthop Res*. 2004;22(6):1296–302.
30. Onambele GN, Burgess K, Pearson SJ. Gender-specific *in vivo* measurement of the structural and mechanical properties of the human patellar tendon. *J Orthop Res*. 2007;25(12):1635–42.
31. Pearson SJ, Burgess K, Onambele GN. Creep and the *in vivo* assessment of human patellar tendon mechanical properties. *Clin Biomech (Bristol, Avon)*. 2007;22(6):712–7.
32. Pearson SJ, Onambele GN. Influence of time of day on tendon compliance and estimations of voluntary activation levels. *Muscle Nerve*. 2006;33(6):792–800.
33. Pearson SJ, Ritchings T, Mohamed AS. The use of normalized cross-correlation analysis for automatic tendon excursion measurement in dynamic ultrasound imaging. *J Appl Biomech*. 2013;29(2):165–73.
34. Revell J, Mirmehdi M, McNally D. Computer vision elastography: speckle adaptive motion estimation for elastography using ultrasound sequences. *IEEE Trans Med Imaging*. 2005;24(6):755–66.